Ferromagnetism, half-metallicity and spin-polarised electronic structures characterisation insights in Ca1–xTixO

Khedidja Korichi, Bendouma Doumi, Allel Mokaddem, Adlane Sayede, Abdelkader Tadjer

Ferromagnetism, half-metallicity and spin-polarised electronic structures characterisation insights in $Ca_{1-x}Ti_xO$

Khedidja Korichi[a], Bendouma Doumi [b,c], Allel Mokaddem[c,d], Adlane Sayede [e] and Abdelkader Tadjer[f]

[a]Laboratory of Physico-Chemical Studies, University of Saida, Saida, Algeria; [b]Faculty of Sciences, Department of Physics, Dr. Tahar Moulay University of Saida, Saida, Algeria; [c]Laboratoire d'Instrumentation et Matériaux Avancés, Centre Universitaire Nour Bachir El Bayadh, El Bayadh, Algérie; [d]Centre Universitaire Nour Bachir El Bayadh, El Bayadh, Algérie; [e]Faculté des Sciences, Unité de Catalyse et Chimie du Solide (UCCS), UMR CNRS 8181, Université d'Artois, Lens, France; [f]Modelling and Simulation in Materials Science Laboratory, Physics Department, Djillali Liabes University of Sidi Bel-Abbes, Sidi Bel-Abbes, Algeria

ABSTRACT

In this study, we have computed the structural, electronic and half-metallic ferromagnetic properties of $Ca_{1-x}Ti_xO$ compounds at concentrations x = 0.125, 0.25, 0.5 and 0.75 by employing the first-principle approaches of density functional theory. The generalised gradient approximation of Wu and Cohen (GGA-WC) is used to calculate the structural parameters, whereas the electronic structures and magnetic properties are characterised by the accurate Tran–Blaha-modified Becke–Johnson potential (TB-mBJ). The lattice constant, bulk modulus and indirect gap of CaO are in good agreement with other theoretical and experimental results. The Ca0.25Ti0.75O at x = 0.75 has metallic ferromagnetic nature. The $Ca_{0.875}Ti_{0.125}$ O, $Ca_{0.75}Ti_{0.25}O$ and Ca0.50Ti0.50O compounds have total magnetic moments of 2 μB per Ti atom with a half-metallic character, a spin polarisation of 100% and a large half-metallic gap of 1.345 eV for x = 0.125. Therefore, the $Ca_{1-x}Ti_xO$ material with a low concentration of Ti is a true half-metallic ferromagnet and seems to be a promising candidate for semiconductor spintronics.

1. Introduction

A modern electronics technology called spintronics has attracted considerable interest in data processing for magnetic memory devices applications, ultra-high density information storage and longer-term design of new electronic components [1]. Spin (or spintronic) electronics [2] exploits the magnetic spin of

electron for the technology of electronics devices; it is originated from the discovery of giant magnetoresistance [3, 4]. Spintronics technology is focused on the simultaneous control and manipulation of the electron charge as well as its magnetic moment (spin) in order to realise substantial applications in memory devices and sensors to improve the performance of new logical and information storage devices [2, 5]. The expected benefit of spintronics over conventional electronics would be non-volatility, increased data processing speed, increased transistor density and reduced power consumption [6].

A revolution has been marked by the integration of spintronics into spintronics devices based on magnetic semiconductors by the possibility of combining the storage and manipulation functions through both magnetic and semiconductor elements [2, 5, 7]. The doped magnetic semiconductors called diluted magnetic semiconductors (DMS) based on II–VI semiconductors are considered as innovative candidates for the development of new spintronics devices. Many researchers have extensively studied these compounds because they exhibit a half-metallic feature [8, 9] and owing to their ferromagnetic stability at temperatures above room temperature [10, 11]. The calcium chalcogenides CaX (X = S, Se, Te) belong to the II–VI type alkaline earth chalcogenides, which are important compounds because of their extensive applications ranging from catalysis to microelectronics as well as in the field of electro- and photo-luminescent devices [12–22]. The CaO calcium oxide wide-bandgap semiconductor is one of the families of calcium chalcogenides, which crystallised in the NaCl-type structure (B1) and undergoes a first-order phase transition from NaCl (B1) phase to the CsCl (B2) structure under high pressure [16–21]. The CaO is considered a potential DMS material for spintronics according to first-principle theoretical studies of Kenmochi et al. [23, 24] and An Dinh et al. [25], which investigated the origin of magnetism and room-temperature ferromagnetism in CaO induced by the substituting effect of non-magnetic carbon (C) and nitrogen (N) impurities. Recently, Jun et al., [26] have predicted new rare-earth half-metallic ferromagnets based on CaO doped with europium (Eu).

The objective of this study is to elucidate the structural, electronic and magnetic properties of CaO under the substituting effect of titanium (Ti) magnetic impurities such as the $Ca_{1-x}Ti_xO$ compounds at concentrations $x = 0.125$, 0.25, 0.5 and 0.75. The calculations of these properties have been made by the first-principle concepts of density functional theory (DFT) [27, 28] within the full-potential linearised augmented plane-wave (FP-LAPW) method [29], the generalised gradient approximation of Wu-Cohen (GGA-WC) [30] and the Tran–Blaha-modified Becke–Johnson (TB-mBJ) exchange potential [31, 32] as implemented in WIEN2k package [33].

2. Computational method and details of calculations

We have performed the calculations of structural, electronic and magnetic properties of $Ca_{1-x}Ti_xO$ compounds at concentrations $x = 0.125$, 0.25, 0.5 and 0.75 by

the use of WIEN2k code [33] within the first-principle computations of DFT [27, 28] theory and FP-LAPW method [29]. The structural parameters are computed by Wu-Cohen gradient generalised gradient approximation (GGA-WC) [30], whereas the appropriate Tran–Blaha-modified Becke–Johnson (TB-mBJ) exchange potential [31, 32] is employed to characterise the magnetic properties, electronic structure and accurate band-gaps.

The wave functions are extended to plane waves in the interstitial zone with $K_{max} = 8.0/R_{MT}$, where the K_{max} presents the largest K vector of plane wave and R_{MT} defines the average radius of muffin-tin sphere. Inside the atomic sphere, we have chosen the value of $l_{max} = 10$ for maximum partial waves. The Fourier charge density is extended up to $G_{max} = 14$ (a.u.)$^{-1}$, where G_{max} is the largest vector in the Fourier expansion. In the Brillouin-zone integration, we have employed the Monkhorst–Pack mesh [34] of $(4 \times 4 \times 4)$ k-points for CaO, $Ca_{0.75}Ti_{0.25}O$ and $Ca_{0.25}Ti_{0.75}O$, $(4 \times 4 \times 2)$ k-points for $Ca_{0.875}Ti_{0.125}O$ and $(4 \times 4 \times 3)$ k-points for $Ca_{0.5}Ti_{0.5}O$.

3. Results and discussions

3.1. Structural properties

The CaO calcium oxide belongs to the family of II–VI type semiconductors, which crystallises in the rocksalt NaCl (B1) structure with space group of $Fm\bar{3}m$ No. 225, where the (Ca) calcium atom occupies the (0, 0, 0) position and the oxygen (O) at (0.5, 0.5, 0.5) site. The $Ca_{1-x}Ti_xO$ compounds at concentrations ($x = 0.125$) and ($x = 0.25$, 0.5 and 0.75) are generated respectively by using the supercells of 16 and 8 atoms. The Ca_7TiO_8 $(1 \times 1 \times 2)$ supercell of 16 atoms is created from Ca_8O_8 structure by substituting one Ca cationic site with Ti impurity. We get the $Ca_{0.875}Ti_{0.125}O$ tetragonal structure with concentration $x = 0.125$ and space group of $P4/mmm$ No. 123. The Ca3TiO4 $(1 \times 1 \times 1)$, $Ca_2Ti_2O_4$ $(1 \times 1 \times 1)$ and $CaTi_3O_4$ $(1 \times 1 \times 1)$ supercells of 8 atoms are obtained by substituting Ca cationic sites respectively with one, two and three Ti impurities. We get the cubic structures of $Ca_{0.75}Ti_{0.25}O$ for $x = 0.25$ and $Ca_{0.25}Ti_{0.75}O$ for $x = 0.75$ with space group of $Pm\bar{3}m$ No 221, and tetragonal structure of $Ca_{0.5}Ti_{0.5}O$ with space group of $P4/mmm$ No. 123.

The optimised structural parameters are determined by fitting the variations of energies as a function of equilibrium volumes using the empirical Murnaghan equation of state [35]. The computed structural properties such as the lattice constants (a), bulk modules (B) and their pressure derivatives (B') of CaO and $Ca_{1-x}Ti_xO$ at concentrations $x = 0.125$, 0.25, 0.5 and 0.75 with other theoretical [36–39] and experimental [40] results are given in Table 1. The lattice constant and the bulk modulus of CaO are close to theoretical values [36] of GGA-WC [30] and appeared to be consistent with the experimental ones [40]. Also, these parameters are improved than that of the results of Refs. [36–38] and

Table 1. Calculated lattice constants (a), bulk modules (B) and their pressure derivatives (B') for CaO and $Ca_{1-x}Ti_xO$ compounds at concentrations x = 0.125, 0.25, 0.5 and 0.75.

Material	a (Å)	B (GPa)	B'	Method
This work				GGA-WC
CaO	4.775	115.23	4.36	
$Ca_{0.875}Ti_{0.125}O$	4.706	119.81	4.27	
$Ca_{0.75}Ti_{0.25}O$	4.640	125.22	4.39	
$Ca_{0.5}Ti_{0.5}O$	4.478	132.56	3.90	
$Ca_{0.25}Ti_{0.75}O$	4.311	166.41	4.30	
Other calculations				
CaO				
	4.777 [36]	116 [36]		GGA-WC
	4.841 [36]	105 [36]		GGA-PBE
	4.843 [37]	107 [37]	4.2 [37]	GGA-PBE
	4.836 [38]	102.3 [38]	4.17 [38]	GGA-PBE
	4.734 [39]	119.54 [39]	4.23 [39]	LDA
	4.8105 [40]	115 [40]	4.1 [40]	Experimental

Ref. [39] calculated respectively by the generalised gradient approximation of Perdew–Burke–Ernzerhof (GGA-PBE) [41] and the local density approximation (LDA) [42]. The better performance of GGA-WC approximation for optimising structural parameters is due to its fourth-order gradient expansion of exchange and correlation functional [30, 43–45]. In addition, Table 1 shows that the lattice parameter decreases with increasing concentration (x) of substituted Ti impurity owing to smaller size of the Ti ionic radius with respect to the Ca. Consequently, the $Ca_{1-x}Ti_xO$ doping compound becomes harder due to the increase in bulk modulus with increasing Ti concentration.

3.2. Spin-polarised electronic structures and half-metallic properties

The results of the lattice parameters found by GGA-WC [30] were used to determine the spin-polarised electronic structures such as the densities of states, the band structures as well as the band-gaps of the compounds under study. Figures 1–5 show the plots of calculated band structures with TB-mBJ [31, 32], respectively for CaO, $Ca_{0.875}Ti_{0.125}O$, $Ca_{0.75}Ti_{0.25}O$, $Ca_{0.5}Ti_{0.5}O$ and $Ca_{0.25}Ti_{0.75}O$. It is clear that Figure 1 exhibits the identical band structure with bandgap for two spins channels, implying that CaO is a semiconductor with indirect band-gap positioned between valence bands maximum and the conduction bands minimum respectively at Γ and X high symmetry points. For high concentration $x = 0.75$, the Fermi level is crossed by overlapping bands, leading to metallic nature for $Ca_{0.25}Ti_{0.75}O$ compound. For concentrations $x = 0.125$, 0.25 and 0.5, the $Ca_{0.875}Ti_{0.125}O$, $Ca_{0.75}Ti_{0.25}O$ and $Ca_{0.5}Ti_{0.5}O$ are semiconductors for spins down, while the spins up are metallic as 3d-Ti bands intersect Fermi level. Thus, these compounds have a half-metallic ferromagnetic character.

The half-metallic ferromagnetic materials are described by two important band-gaps; the first is called the half-metallic ferromagnetic gap localised

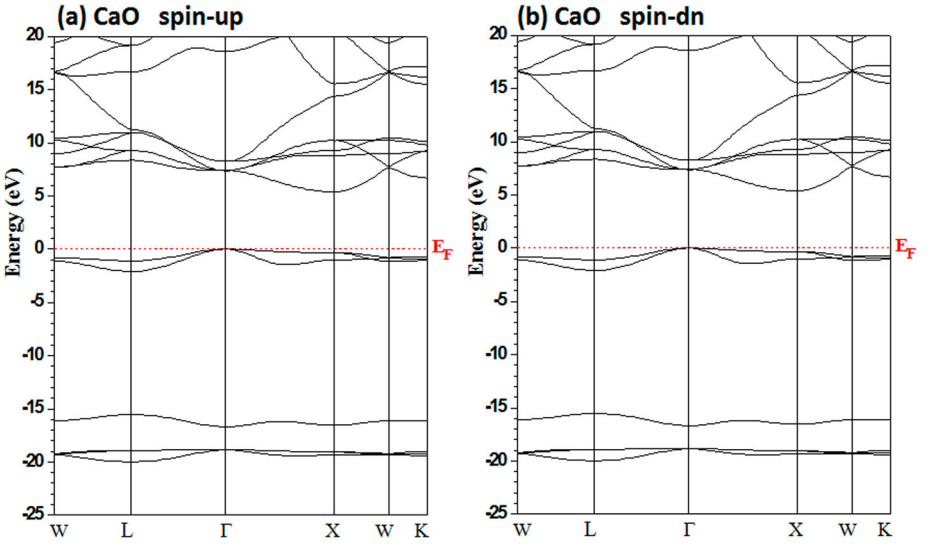

Figure 1. Band structures of CaO. **(a)** Majority spins (*up*) and **(b)** Minority spins (*dn*).

around Fermi level between the valence bands maximum and the conduction bands minimum, and the second is known as the half-metallic gap, which is defined as the absolute value of the maximum energy of valence bands of majority (minority)-spin or the minimum between the minimum energy of conduction bands of majority (minority)-spin with respect to the Fermi level [46, 47]. Table 2 summarises the computed values of half-metallic ferromagnetic gaps (G_{HMF}) and half-metallic gaps (G_{HM}) for $Ca_{1-x}Ti_xO$ at

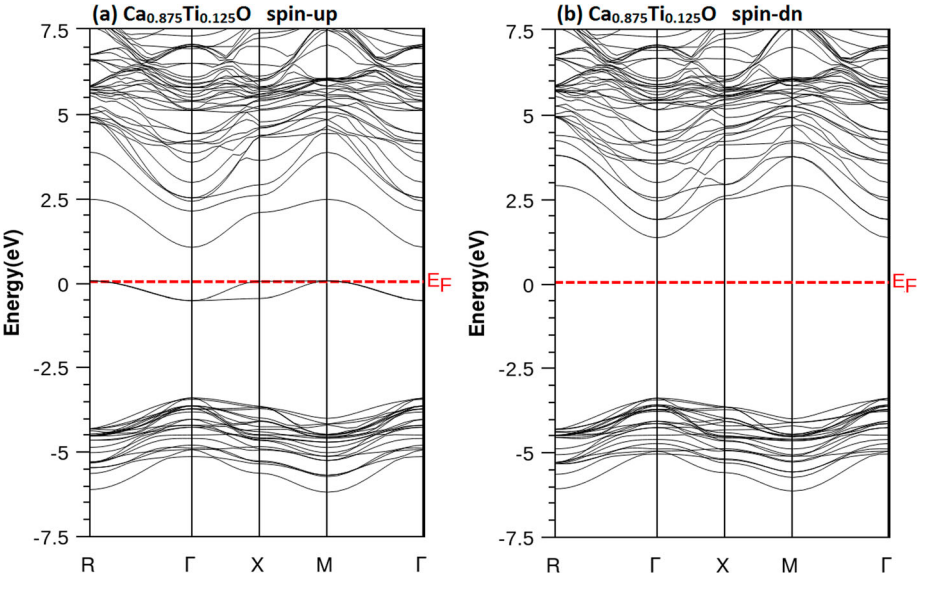

Figure 2. Band structures of $Ca_{0.875}Ti_{0.125}O$. **(a)** Majority spins (*up*) and **(b)** Minority spins (*dn*).

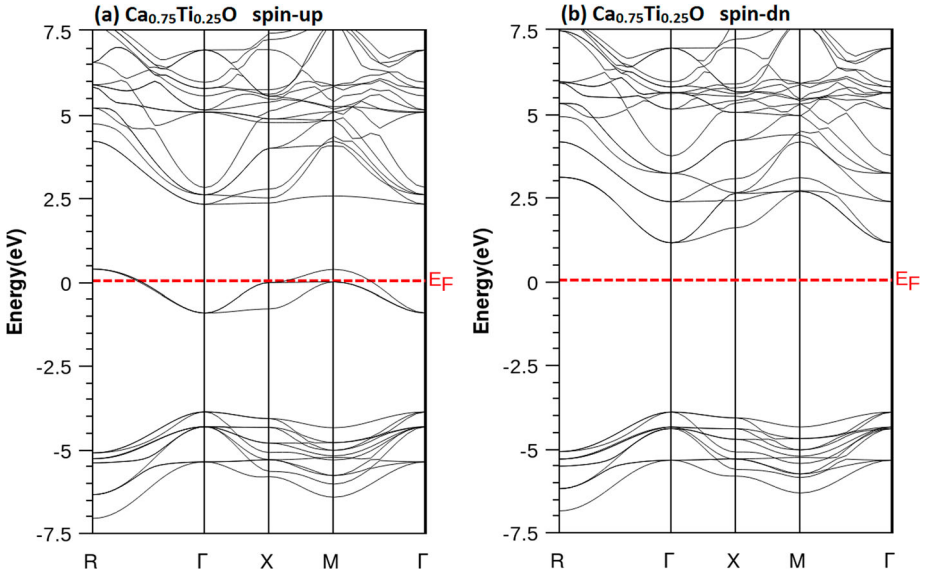

Figure 3. Band structures of $Ca_{0.75}Ti_{0.25}O$. **(a)** Majority spins (*up*) and **(b)** Minority spins (*dn*).

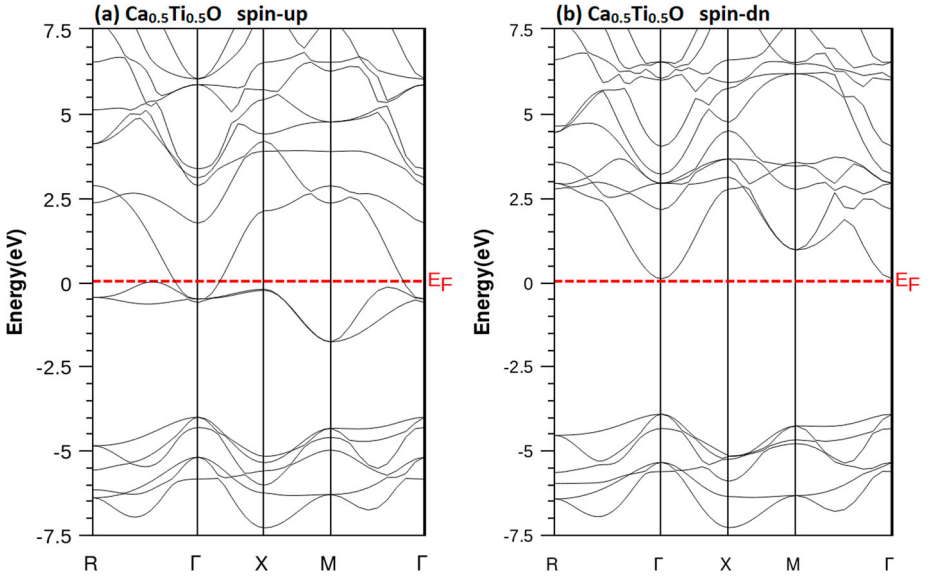

Figure 4. Band structures of $Ca_{0.5}Ti_{0.5}O$. **(a)** Majority spins (*up*) and **(b)** Minority spins (*dn*).

concentrations $x = 0.125$, 0.25 and 0.5, and indirect gap ($E^{\Gamma X}$) of CaO with other theoretical [39, 48] and experimental [49] values. Due to the accurate TB-mBJ potential for computing electronic structures, our calculated indirect gap of 5.38 eV for CaO is in good agreement with the value of 5.35 eV [48] found by the same potential and it is better than that of the results of Refs. [39, 48] and Ref. [48] using GGA-PBE [41] and LDA [42] approximations,

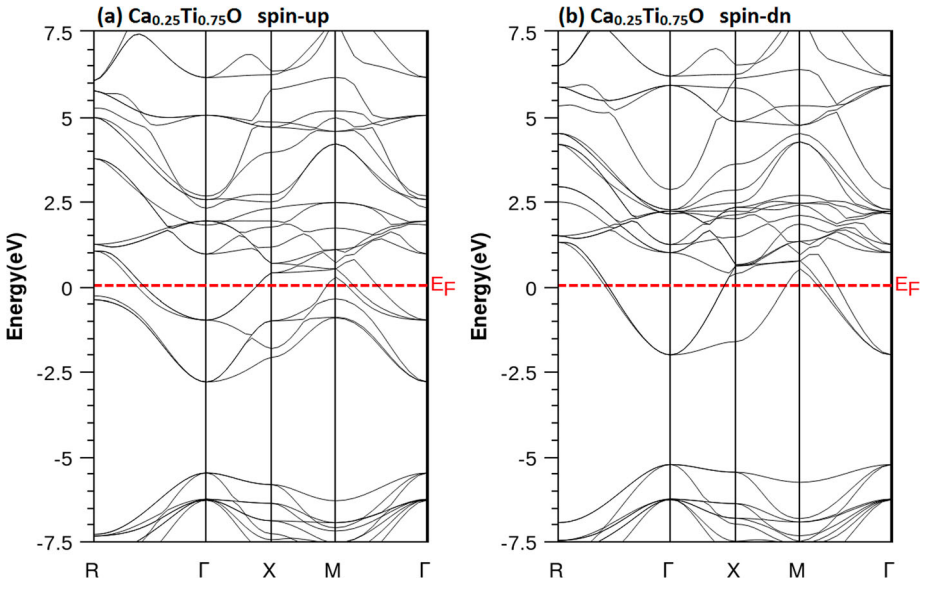

Figure 5. Band structures of $Ca_{0.25}Ti_{0.75}O$. **(a)** Majority spins (*up*) and **(b)** Minority spins (*dn*).

Table 2. Calculated indirect band gap ($E^{\Gamma X}$) of CaO, half-metallic ferromagnetic (HMF) (G_{HMF}) and half-metallic gap (G_{HM}) of minority-spin bands for $Ca_{1-x}Ti_xO$ at concentrations x = 0.125, 0.25 and 0.5.

Material	G_{HMF} (eV)	G_{HM} (eV)	$E^{\Gamma X}$ (eV)	Method
This work				
CaO			5.38	TB-mBJ
$Ca_{0.875}Ti_{0.125}O$	4.742	1.345		TB-mBJ
$Ca_{0.75}Ti_{0.25}O$	5.049	1.134		TB-mBJ
$Ca_{0.5}Ti_{0.5}O$	4.019	0.094		TB-mBJ
Other calculations				
CaO				
			3.658 [38]	GGA-PBE
			3.67 [48]	GGA-PBE
			3.49 [48]	LDA
			5.35 [48]	TB-mBJ
			7.00 [49]	Experimental

respectively. The minority spins of $Ca_{0.875}Ti_{0.125}O$, $Ca_{0.75}Ti_{0.25}O$ and $Ca_{0.5}Ti_{0.5}O$ compounds are characterised by direct half-metallic ferromagnetic (HMF) gaps of 4.742, 5.049 and 4.019 eV located at Γ high symmetry point. However, the conduction bands minimum of minority spins moves to lower energies near Fermi level due to the widening of 3d-Ti shells in the gap as the concentration of Ti increases. Owing to broadening of 3d-Ti bands in the gap, the bottom of conduction bands overlaps with the Fermi level and hence the $Ca_{0.25}Ti_{0.75}O$ compound at concentration $x = 0.75$ becomes metallic.

The HM gap or flip-gap occurs between the conduction bands minimum and Fermi level, which defines the lowest energy to create an electron in conduction

band [45]. It is an important property that characterises the half-metallic materials for spintronics applications [46, 47]. The $Ca_{0.875}Ti_{0.125}O$, $Ca_{0.75}Ti_{0.25}O$ and $Ca_{0.5}Ti_{0.5}O$ compounds have half-metallic (HM) gaps of 1.345, 1.134 and 0.094 eV, respectively. We have noticed that the HM gap decreases with increasing Ti concentration because conduction bands minimum shifted towards the Fermi level. Besides, the $Ca_{0.875}Ti_{0.125}O$ at concentration $x = 0.125$ has higher HM gap of 1.345. Consequently, the $Ca_{1-x}Ti_xO$ material doped with a lower Ti concentration is a perfect half-metallic ferromagnetic with a spin polarisation of 100%, making it a suitable candidate for spintronics.

Furthermore, the total and partial densities of states (DOS) of $Ca_{0.875}Ti_{0.125}O$, $Ca_{0.75}Ti_{0.25}O$, $Ca_{0.5}Ti_{0.5}O$ and $Ca_{0.25}Ti_{0.75}O$ are given by Figures 6–9. The plots of DOS show that the $Ca_{0.875}Ti_{0.125}O$, $Ca_{0.75}Ti_{0.25}O$, $Ca_{0.5}Ti_{0.5}O$ materials have a half-metallic ferromagnetic character described by the metallic nature of spins up and the semiconductor feature of spins down, where the metallic property of majority-spin states results from large p-d hybridisation between p states of oxygen (O) and 3d states of Ti atom. From Figure 9, we have depicted that the $Ca_{0.25}Ti_{0.75}O$ at concentration $x = 0.75$ is metallic because the DOS of both majority and minority-spin states dominate the Fermi level. The partial DOS of $Ca_{0.875}Ti_{0.125}O$, $Ca_{0.75}Ti_{0.25}O$, $Ca_{0.5}Ti_{0.5}O$ show that the 3d states of Ti impurity are separated into two levels such as the three low-lying t_{2g} (d_{xy}, d_{xz}, d_{yz}) partially filled states and two high-lying e_g (d_{z^2}, $d_{x^2-y^2}$) unfilled states. This is due to crystal field produced by the surroundings oxygen (O) ions. We have noticed that the e_g states occur above t_{2g} states, meaning that the Ti atom is sited in an octahedral crystal field environment [43, 50].

The metallic nature and ferromagnetism in $Ca_{1-x}Ti_xO$ doping materials are originated from the itinerant electrons of localised 3d-Ti majority-spin states. For minority spin, the bonding states of valence band are originated principally from DOS of p-O states, while the empty 3d-Ti states are located at the bottom of conduction bands. Therefore, the density of states are absent around Fermi level and a band gap is formed between the maximum and minimum of valence and conduction bands, respectively. In addition, the spin polarisation (P) of a half-metallic material is measured from the contributions of total DOS of spins up $N\uparrow(E_F)$ and spins down $N\downarrow(E_F)$ at Fermi level (E_F); it is given by the following expression [51]:

$$P = \frac{N\uparrow(E_F) - N\downarrow(E_F)}{N\uparrow(E_F) + N\downarrow(E_F)} \tag{1}$$

the spin polarisation $P = 1$ of the $Ca_{1-x}Ti_xO$ at concentrations $x = 0.125$, 0.25 and 0.5 because the total DOS of minority spins $N\downarrow(E_F)$ equal zero. Therefore, the $Ca_{0.875}Ti_{0.125}O$, $Ca_{0.75}Ti_{0.25}O$, $Ca_{0.5}Ti_{0.5}O$ compounds are half-metallic ferromagnets with spin polarisation of 100%.

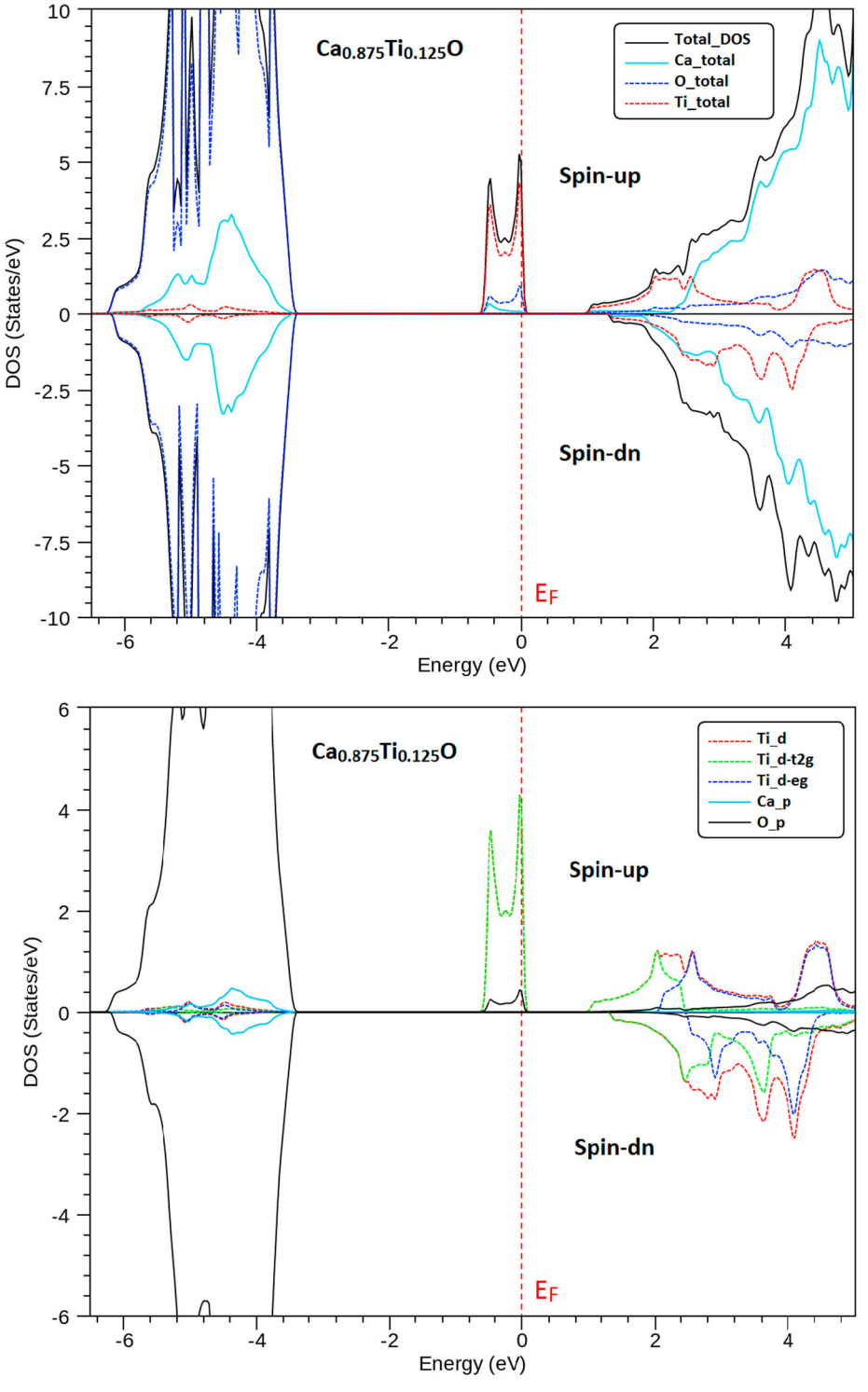

Figure 6. Spin-polarised total and partial densities of states (DOS) of $Ca_{0.875}Ti_{0.125}O$.

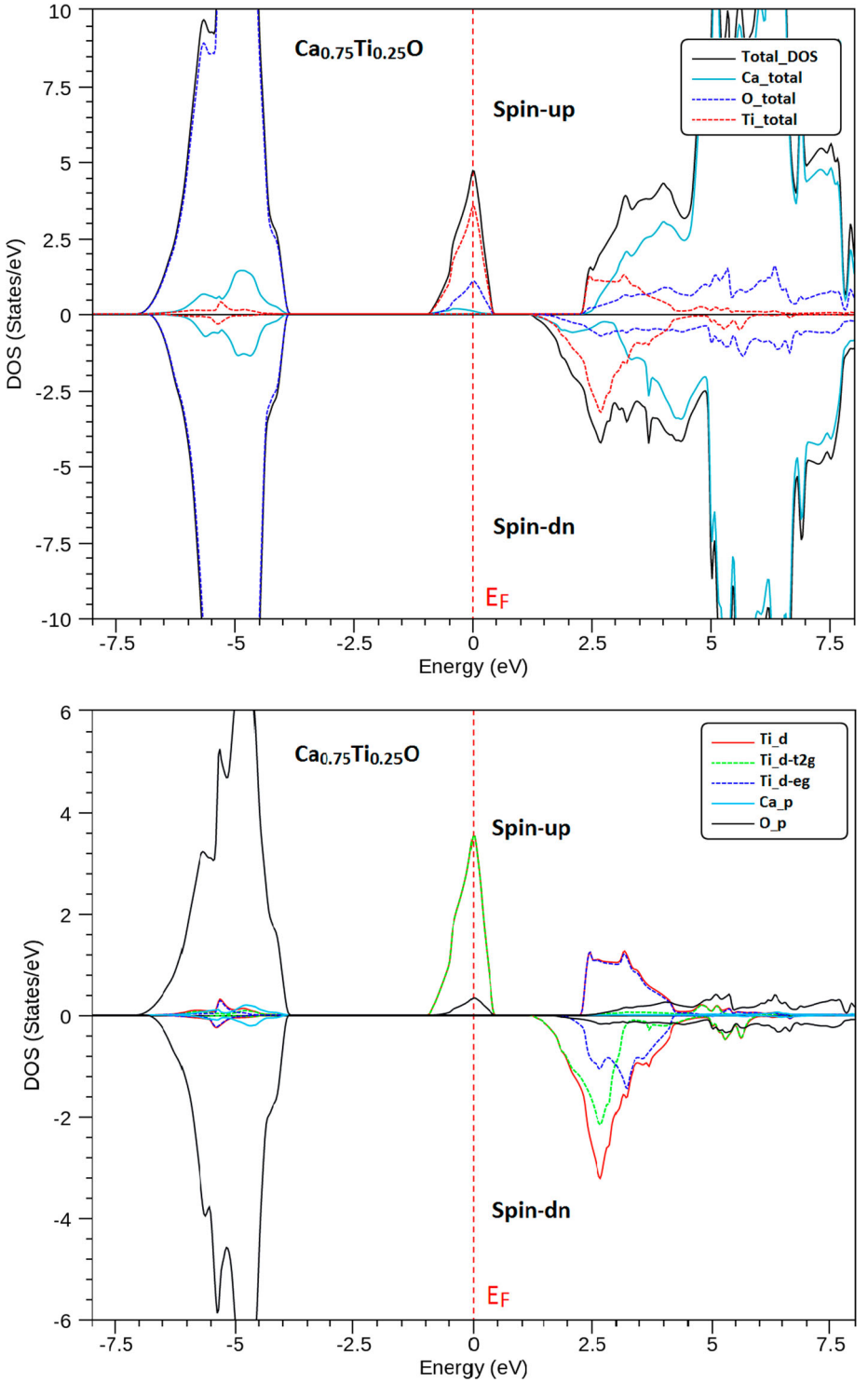

Figure 7. Spin-polarised total and partial densities of states (DOS) of $Ca_{0.75}Ti_{0.25}O$.

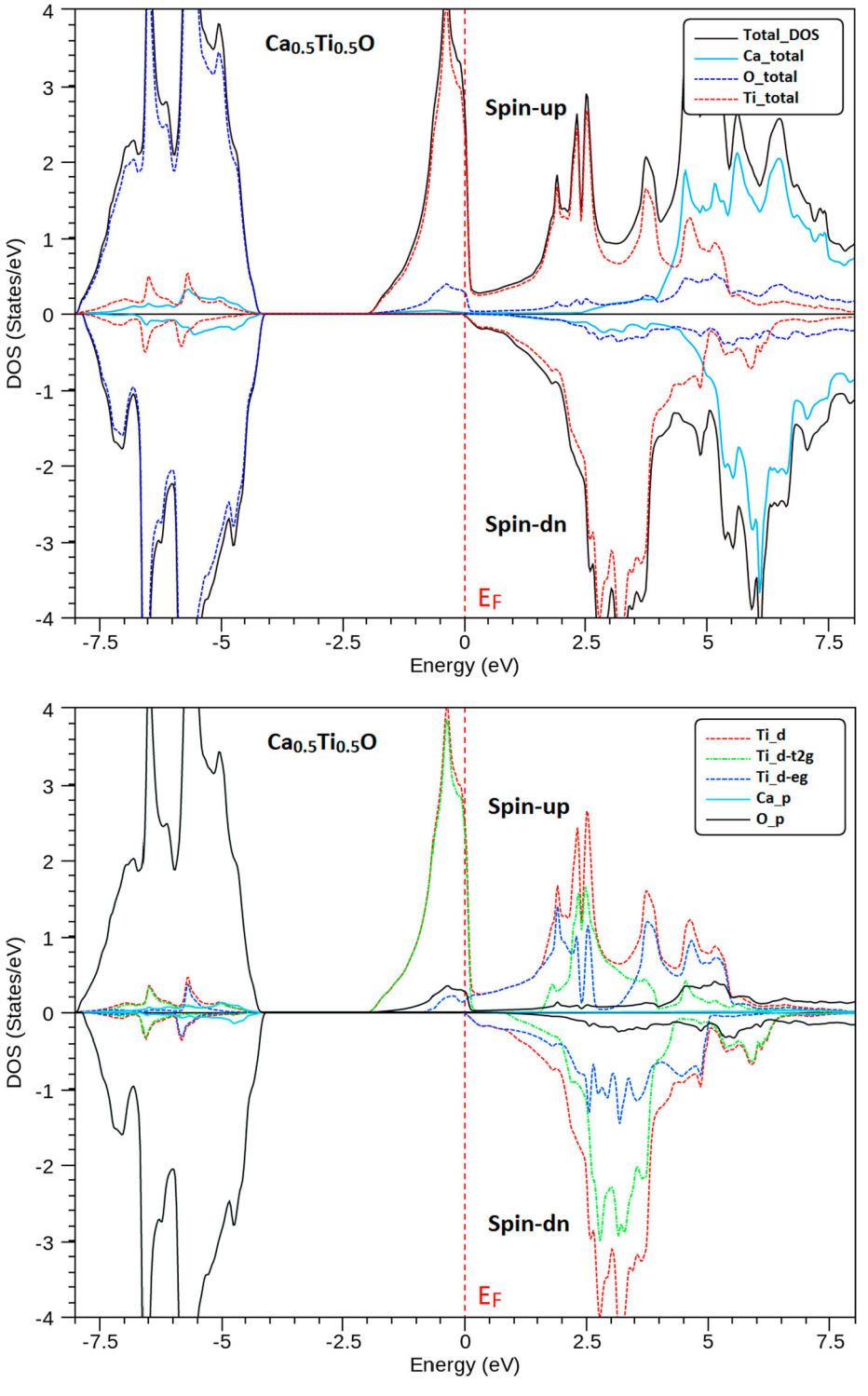

Figure 8. Spin-polarised total and partial densities of states (DOS) of $Ca_{0.5}Ti_{0.5}O$.

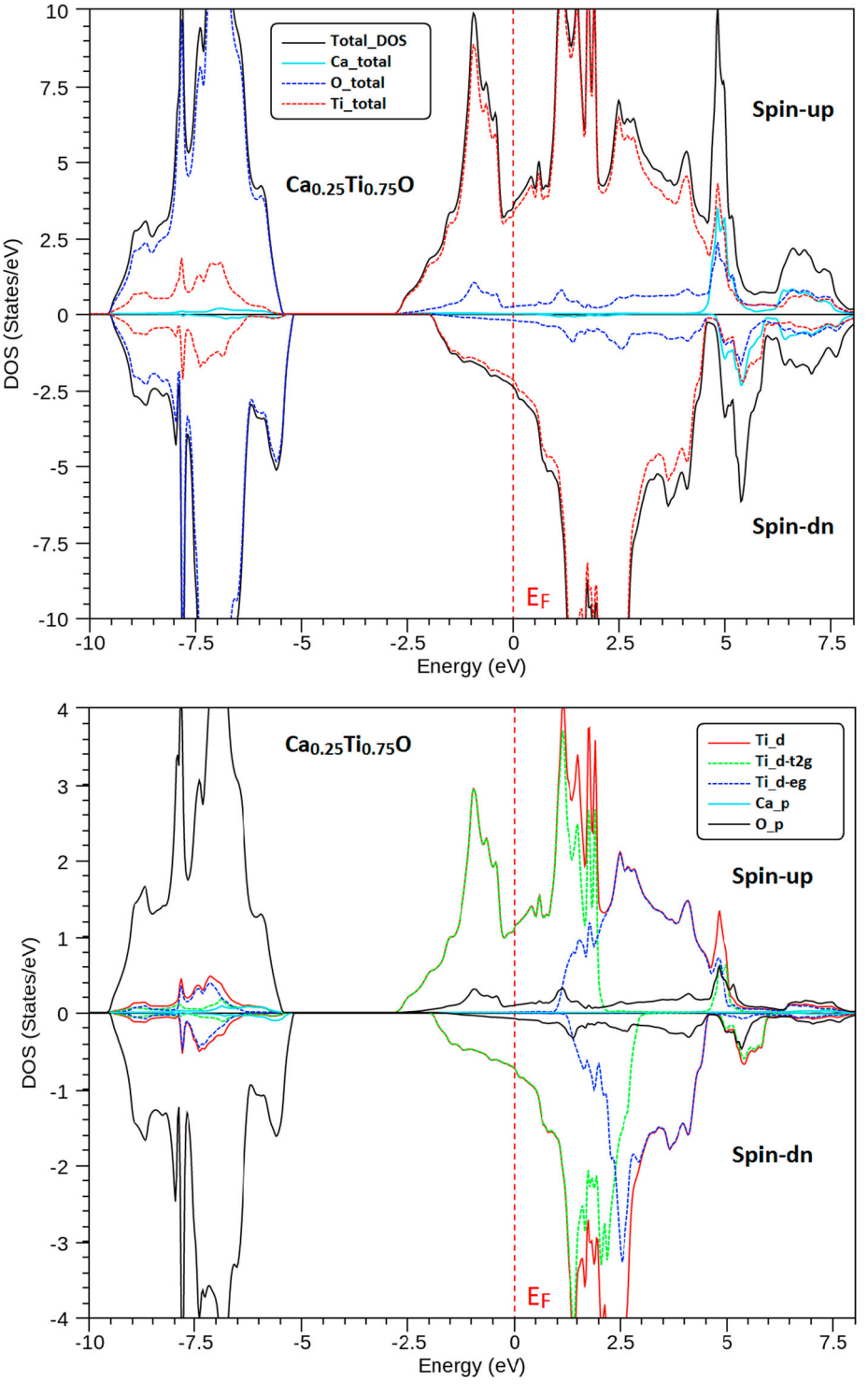

Figure 9. Spin-polarised total and partial densities of states (DOS) of $Ca_{0.25}Ti_{0.75}O$.

3.3. Magnetic properties

3.3.1. Magnetic moments

In the diluted magnetic semiconductors, the ferromagnetic state stability is originated from the double exchange mechanism when the 3d states are partially filled [52, 53]. According to this rule, the 3d unfilled states of Ti transition metal in the $Ca_{1-x}Ti_xO$, suggest the stability of ferromagnetic state arrangement related to the double exchange mechanism [54]. The origin of ferromagnetism in $Ca_{1-x}Ti_xO$ materials is due to the itinerant electrons of 3d-Ti partially occupied levels. For the $Ca_{1-x}Ti_xO$ systems at concentrations $x = 0.125$, 0.25 and 0.5, the Ti ($4s^2$ $3d^2$) impurity occupies the Ca site and provides two electrons to host valence bands, resulting in Ti^{+2} ($4s^0$ $3d^2$) ion. Therefore, the 3d states keep two unpaired electrons that generate a total magnetic moment of 2 μ_B per Ti ion, where the μ_B is the Bohr magneton. However, the strong p-d exchange interactions arise between p-O and 3d-Ti states, which reduce the magnetic moment of Ti less than 2 μ_B and induce less important partial magnetic moments for Ca and O atoms. The calculated total and partial magnetic moments of $Ca_{1-x}Ti_xO$ compounds at concentrations $x = 0.125$, 0.25, 0.5 and 0.75 are given in Table 3. The total magnetic moments equal to 2 μ_B per Ti atom for concentrations $x = 0.125$, 0.25, 0.5, confirming that the $Ca_{0.875}Ti_{0.125}O$, $Ca_{0.75}Ti_{0.25}O$, $Ca_{0.5}Ti_{0.5}O$ are half-metallic, but the $Ca_{0.75}Ti_{0.25}O$ compound at higher concentration $x = 0.75$ is metallic ferromagnetic with total magnetic moment of 1.33 μ_B per Ti atom. On the other hand, the ferromagnetic interactions occur between the positive magnetic moments of Ti, Ca and O for $Ca_{1-x}Ti_xO$ at concentrations $x = 0.125$, 0.5 and 0.75, and between positive Ca and Ti magnetic spins for $Ca_{1-x}Ti_xO$ at $x = 0.25$. In contrast, the anti-ferromagnetic interaction is formed between positive Ti magnetic spin and negative magnetic moment of O atom for $Ca_{1-x}Ti_xO$ at $x = 0.25$.

3.3.2. Exchange constants and exchange splittings

In this section, we have computed the exchange constants to investigate the exchange couplings between valence and conduction bands with the 3d-Ti magnetic atoms. The exchange constants are determined by the use of the

Table 3. Calculated total and partial magnetic moments at Ti, Ca and O sites and in the interstitial site of $Ca_{1-x}Ti_xO$ compounds at concentrations $x = 0.125$, 0.25, 0.5 and 0.75.

Material	Total (μ_B)	Ti (μ_B)	Ca (μ_B)	O (μ_B)	Interstitial (μ_B)
$Ca_{0.875}Ti_{0.125}O$	2	1.568	0.016	0.041	0.375
$Ca_{0.75}Ti_{0.25}O$	2	1.498	0.037	−0.072	0.537
$Ca_{0.5}Ti_{0.5}O$	4	3.036	0.037	0.044	0.883
$Ca_{0.25}Ti_{0.75}O$	3.988	2.274	0.017	0.15	1.547

mean-field theory with the following expressions [55, 56]:

$$N_0\alpha = \frac{\Delta E_c}{x\langle s\rangle} \tag{2}$$

$$N_0\beta = \frac{\Delta E_v}{x\langle s\rangle} \tag{3}$$

where the $\Delta E_c = E_c^{\downarrow} - E_c^{\uparrow}$ and $\Delta E_v = E_v^{\downarrow} - E_v^{\uparrow}$ are the valence and conduction band-edge spin-splittings at Γ high symmetry point for $Ca_{1-x}Ti_xO$ at concentrations $x = 0.125$, 0.25 and 0.5, respectively. The $\langle s\rangle$ represents the half total magnetic moment per Ti atom [55] and the x correspond to the concentration of Ti (Table 4).

The $N_0\alpha$ constant defines the exchange coupling between the 3d-Ti levels and the *s*-type conduction bands, whereas the exchange coupling between the 3d-Ti levels and the *p*-type valence bands is explained by the $N_0\beta$ parameter. For $Ca_{1-x}Ti_xO$ compounds at concentrations $x = 0.125$, 0.25 and 0.5, the positive values of $N_0\beta$ reflect the p-d anti-ferromagnetic couplings between valence bands and 3d levels as shown in Table 4. The $N_0\alpha$ parameter is positive for concentration $x = 0.125$ and it is negative for $x = 0.25$ and 0.5, indicating that the interaction between 3d-Ti levels and valence bands is ferromagnetic for $Ca_{0.875}Ti_{0.125}O$ and it is anti-ferromagnetic for $Ca_{0.75}Ti_{0.25}O$ and $Ca_{0.5}Ti_{0.5}O$ compounds. Besides, the typical attraction in the half-metallic ferromagnetic $Ca_{1-x}Ti_xO$ compounds is determined from the indirect $\Delta_x(pd) = E_v^{\downarrow} - E_v^{\uparrow}$ exchange splitting that represents the difference between $E_v^{\downarrow}$and $E_v^{\uparrow}$ energies of valence band maximums respectively for spins down and spins up. The indirect exchange splittings of $Ca_{0.875}Ti_{0.125}O$, $Ca_{0.75}Ti_{0.25}O$, $Ca_{0.5}Ti_{0.5}O$ are −3.40, −3.91 and −3.93 eV, respectively, indicating that spin-polarised $Ca_{1-x}Ti_xO$ materials exhibit an important feature for the spins down, which have a effective nature of potential compared to spins up [57–59].

Furthermore, we have characterised the ferromagnetism in the $Ca_{0.875}Ti_{0.125}O$, $Ca_{0.75}Ti_{0.25}O$ and $Ca_{0.5}Ti_{0.5}O$ compounds by computing the magnitudes of the crystal field and direct exchange splitting. The crystal field energy $\Delta E_{CF} = E_{eg} - E_{t2g}$ is calculated from the difference energies between of e_g and t_{2g} levels. The direct exchange splitting $\Delta_x(d) = d\downarrow - d\uparrow$ corresponds to the energy separation between the peaks of d-Ti ($d\downarrow$) and d-Ti ($d\uparrow$) respectively for spins down and spins up. From the partial DOS, we have depicted that the

Table 4. Computed conduction band-edge ΔE_c (eV) and valence band-edge ΔE_v (eV) spin-splittings, sp-d exchange constants $N_0\alpha$ and $N_0\beta$, crystal field ΔE_{CF} (eV) and direct exchange $\Delta_x(d)$ (eV) splittings for $Ca_{1-x}Ti_xO$ at concentrations $x = 0.125$, 0.25 and 0.5.

Material	ΔE_c	ΔE_v	$N_0\alpha$	$N_0\beta$	ΔE_{CF}	$\Delta_x(d)$
$Ca_{0.875}Ti_{0.125}O$	0.30	−2.87	1.20	−11.48	4.46	4.14
$Ca_{0.75}Ti_{0.25}O$	−1.17	−2.98	−2.34	−5.96	2.48	3.24
$Ca_{0.5}Ti_{0.5}O$	−1.65	−3.42	−1.65	−3.42	2.29	3.54

peaks of t_{2g} and 3d states of spins up are situated at the same level of energy for the concentrations $x = 0.25$ and 0.5. In contrast, for the d-Ti states of spins down with respect to the e_g states of spins up, the d-Ti states are more dominated than that of the e_g states for the concentrations $x = 0.25$ and 0.5, but for the smaller concentration $x = 0.125$, the pick of the e_g majority-spin states have a higher energy compared to the d-Ti minority-spin states. These behaviours are reflected by the energies of crystal field and direct exchange splittings (ΔE_{CF} and $\Delta_x(d)$) of (4.46 and 4.41), (2.48 and 3.24) and (2.29 and 3.24 eV) respectively for the $Ca_{0.875}Ti_{0.125}O$, $Ca_{0.75}Ti_{0.25}O$ and $Ca_{0.5}Ti_{0.5}O$ compounds. Consequently, the crystal field splitting is more dominated than that of direct exchange splitting for $Ca_{0.875}Ti_{0.125}O$ at low concentration $x = 0.125$, while for the $Ca_{0.75}Ti_{0.25}O$ and $Ca_{0.5}Ti_{0.5}O$ compounds the crystal field is confined in the direct exchange splitting. We understand that the ferromagnetism is more favourable by the crystal field splitting in the $Ca_{0.875}Ti_{0.125}O$ compound at the lower concentration $x = 0.125$.

4. Conclusion

The structural, spin-polarised electronic structures and magnetic properties of Ti-doped CaO semiconductor such as the $Ca_{1-x}Ti_xO$ compounds at various concentrations $x = 0.125$, 0.25, 0.5 and 0.75 were studied by using the WIEN2k code based on the GGA-WC approximation and the TB-mBJ potential. The structural parameters and indirect band gap of CaO computed respectively by GGA-WC and TB-mBJ potentials show a good concordance with other recent theoretical calculations found by the same potentials. The lattice parameter of $Ca_{1-x}Ti_xO$ is reduced than that of the CaO, which decreases with increasing concentration of Ti due to the difference between the sizes of ionic radii of Ca and Ti atoms. The $Ca_{0.25}Ti_{0.75}O$ at high concentration $x = 0.75$ has a metallic ferromagnetic nature. For other concentrations, the $Ca_{0.875}Ti_{0.125}O$, $Ca_{0.75}Ti_{0.25}O$, $Ca_{0.5}Ti_{0.5}O$ are perfect half-metallic ferromagnets with a spin polarisation of 100% and a large half-metallic gap of 1.345 eV for $x = 0.125$. The ferromagnetism is explained by both crystal field and direct exchange splittings, where it is more appropriate by the contribution of crystal field splitting mechanism for $Ca_{1-x}Ti_xO$ at low concentration $x = 0.125$. Therefore, $Ca_{1-x}Ti_xO$ material doped with lower concentration of titanium is considered as potential candidate for exploration in the future spintronics applications.

References

[1] J. De Boeck, W. Van Roy, J. Das, V. Motsnyi, Z. Liu, L. Lagae, H. Boeve, K. Dessein and G. Borghs, *Technology and materials issues in semiconductor-based magnetoelectronics*, Semicond. Sci. Tech 17 (2002), pp. 342.

[2] S. Wolf, D. Awschalom, R. Buhrman, J. Daughton, S. Von Molnar, M. Roukes, A.Y. Chtchelkanova and D. Treger, *Spintronics: A spin-based electronics vision for the future*. Science 294 (2001), pp. 1488–1495.

[3] M.N. Baibich, J.M. Broto, A. Fert, F.N. Van Dau, F. Petroff, P. Etienne, G. Creuzet, A. Friederich and J. Chazelas, *Giant magnetoresistance of (001) Fe/(001) Cr magnetic superlattices*. Phys. Rev. Lett 61 (1988), pp. 2472.

[4] G. Binasch, P. Grünberg, F. Saurenbach and W. Zinn, *Enhanced magnetoresistance in layered magnetic structures with antiferromagnetic interlayer exchange*. Phys. Rev. B 39 (1989), pp. 4828.

[5] I. Žutić, J. Fabian and S.D. Sarma, *Spintronics: Fundamentals and applications*. Rev. Mod. Phys 76 (2004), pp. 323.

[6] M. Kaminska, A. Twardowski and D. Wasik, *Mn and other magnetic impurities in GaN and other III–V semiconductors–perspective for spintronic applications*. J. Mater. Sci-Mater. El 19 (2008), pp. 828–834.

[7] H. Ohno, *Making nonmagnetic semiconductors ferromagnetic*. Science 281 (1998), pp. 951–956.

[8] B. Doumi, A. Tadjer, F. Dahmane, A. Djedid, A. Yakoubi, Y. Barkat, M.O. Kada, A. Sayede and L. Hamada, *First-principles investigation of half-metallic ferromagnetism in V-doped BeS, BeSe, and BeTe*. J. Supercond. Nov. Magn 27 (2014), pp. 293–300.

[9] A. Mokaddem, B. Doumi, A. Sayede, D. Bensaid, A. Tadjer and M. Boutaleb, *Investigations of electronic structure and half-metallic ferromagnets in Cr-doped zinc-blende BeS semiconductor*. J. Supercond. Nov. Magn 28 (2015), pp. 157–164.

[10] K. Sato and H. Katayama-Yoshida, *Material design of GaN-based ferromagnetic diluted magnetic semiconductors*. Jpn. J. Appl. Phys 40 (2001), pp. L485.

[11] S.Y. Wu, H. Liu, L. Gu, R. Singh, L. Budd, M. Van Schilfgaarde, M. McCartney, D.J. Smith and N. Newman, *Synthesis, characterization, and modeling of high quality ferromagnetic Cr-doped AlN thin films*. Appl. Phys. Lett 82 (2003), pp. 3047–3049.

[12] R.P. Rao, *The preparation and thermoluminescence of alkaline earth sulphide phosphors*. J. Mater. Sci 21 (1986), pp. 3357–3386.

[13] J. Versluys, D. Poelman, D. Wauters and R. Van Meirhaeghe, *Photoluminescent and structural properties of CaS: Pb electron beam deposited thin films*. J Phys-Condens Mat 13 (2001), pp. 5709.

[14] S. Hakamata, M. Ehara, H. Kominami, Y. Nakanishi and Y. Hatanaka, *Preparation of CaS: Cu, F thin-film electroluminescent devices with an emission including purple region*. Appl. Surf. Sci 244 (2005), pp. 469–472.

[15] A. Kravtsova, I. Stekhin, A. Soldatov, X. Liu and M. Fleet, *Electronic structure of M S (M = Ca, Mg, Fe, Mn): X-ray absorption analysis*. Phys. Rev. B 69 (2004), pp. 134109.

[16] R. Jeanloz and T.J. Ahrens, *Equations of state of FeO and CaO*. Geophys. J. Int 62 (1980), pp. 505–528.

[17] H. Zimmer, H. Winzen and K. Syassen, *High-pressure phase transitions in CaTe and SrTe*. Phys. Rev. B 32 (1985), pp. 4066.

[18] P. Richet, H.K. Mao and P.M. Bell, *Static compression and equation of state of CaO to 1.35 Mbar*. J. Geophys. Res 93 (1988), pp. 15279–15288.

[19] H. Luo, R.G. Greene, K. Ghandehari, T. Li and A.L. Ruoff, *Structural phase transformations and the equations of state of calcium chalcogenides at high pressure*. Phys. Rev. B 50 (1994), pp. 16232.
[20] T. Yamanaka, K. Kittaka and T. Nagai, *B1-B2 transition in CaO and possibility of CaSiO3-perovskite decomposition under high pressure*. J. Miner. Petrol. Sci 97 (2002), pp. 144–152.
[21] S. Speziale, S.R. Shieh, and T.S. Duffy, *High-pressure elasticity of calcium oxide: A comparison between Brillouin spectroscopy and radial X-ray diffraction*. J. Geophys. Res 111 (B2) (2006), p. B02203.
[22] G. Murtaza, R. Khenata, A. Safeer, Z. Alahmed and S.B. Omran, *Shift of band gap from indirect to direct and optical response of CaO by doping S, Se, Te*, Comp. Mater. Sci 91 (2014), pp. 43–49.
[23] K. Kenmochi, M. Seike, K. Sato, A. Yanase and H. Katayama-Yoshida, *New class of diluted ferromagnetic semiconductors based on CaO without transition metal elements*. Jpn. J. Appl. Phys 43 (2004), pp. L934.
[24] K. Kemmochi, M. Seike, K. Sato, A. Yanase and H. Katayama-Yoshida, *New class of high-TC diluted ferromagnetic semiconductors based on CaO without transition metal elements*. J. Supercond 18 (2005), pp. 37–40.
[25] V. An Dinh, M. Toyoda, K. Sato and H. Katayama-Yoshida, *Exchange interaction and TC in alkaline-earth-metal-oxide-based DMS without magnetic impurities: First principle pseudo-SIC and Monte Carlo calculation*. J. Phys. Soc. Jpn 75 (2006), pp. 093705.
[26] L. Jun, Y. Xiao-Lan and K. Wei, *Research on new rare-earth half-metallic ferromagnets X0. 75Eu0. 25O (X = Ca, Sr and Ba) based on the first-principles calculations*. Solid State Commun 242 (2016), pp. 11–15.
[27] P. Hohenberg and W. Kohn, *Inhomogeneous electron gas*. Phys. Rev 136 (1964), pp. B864.
[28] W. Kohn and L.J. Sham, *Self-consistent equations including exchange and correlation effects*. Phys. Rev 140 (1965), pp. A1133.
[29] D.J. Singh and L. Nordstrom, *Planewaves, Pseudopotentials, and the LAPW Method*, Springer Science & Business Media, New York, 2006.
[30] Z. Wu and R.E. Cohen, *More accurate generalized gradient approximation for solids*. Phys. Rev. B 73 (2006), pp. 235116.
[31] F. Tran and P. Blaha, *Accurate band gaps of semiconductors and insulators with a semilocal exchange-correlation potential*. Phys. Rev. Lett 102 (2009), pp. 226401.
[32] D. Koller, F. Tran and P. Blaha, *Merits and limits of the modified Becke-Johnson exchange potential*. Phys. Rev. B 83 (2011), pp. 195134.
[33] P. Blaha, K. Schwarz, G.K. Madsen, D. Kvasnicka and J. Luitz, in *WIEN2k, An Augmented Plane Wave + Local Orbitals Program for Calculating Crystal Properties*, K. schwarz, ed., Techn. Universitaet Wien, Wien, 2001.
[34] H.J. Monkhorst and J.D. Pack, *Special points for Brillouin-zone integrations*. Phys. Rev. B 13 (1976), pp. 5188.
[35] F. Murnaghan, *The compressibility of media under extreme pressures*. Proc. Natl. Acad. Sci. USA 30 (1944), pp. 244.
[36] F. Tran, R. Laskowski, P. Blaha and K. Schwarz, *Performance on molecules, surfaces, and solids of the Wu-Cohen GGA exchange-correlation energy functional*. Phys. Rev. B 75 (2007), pp. 115131.
[37] A.J. Cinthia, G.S. Priyanga, R. Rajeswarapalanichamy and K. Iyakutti, *Structural, electronic and mechanical properties of alkaline earth metal oxides MO (M = Be, Mg, Ca, Sr, Ba)*. J. Phys. Chem. Solids 79 (2015), pp. 23–42.

[38] M.M.A. Salam, *Theoretical study of CaO, CaS and CaSe via first-principles calculations*. Results Phys 10 (2018), pp. 934–945.
[39] J.A. Santana, J.T. Krogel, P.R. Kent and F.A. Reboredo, *Cohesive energy and structural parameters of binary oxides of groups IIA and IIIB from diffusion quantum Monte Carlo*. J. Chem. Phys 144 (2016), pp. 174707.
[40] J. Mammone, H. Mao and P. Bell, *Equations of state of CaO under static pressure conditions*. Geophys. Res. Lett 8 (1981), pp. 140–142.
[41] J.P. Perdew, K. Burke and M. Ernzerhof, *Generalized gradient approximation made simple*. Phys. Rev. Lett 77 (1996), pp. 3865.
[42] J.P. Perdew and A. Zunger, *Self-interaction correction to density-functional approximations for many-electron systems*. Phys. Rev. B 23 (1981), pp. 5048.
[43] B. Doumi, A. Mokaddem, L. Temimi, N. Beldjoudi, M. Elkeurti, F. Dahmane, A. Sayede, A. Tadjer and M. Ishak-Boushaki, *First-principle investigation of half-metallic ferromagnetism in octahedrally bonded Cr-doped rock-salt SrS, SrSe, and SrTe*. Eur. Phys. J. B 88 (2015), pp. 93.
[44] M. Sajjad, S. Manzoor, H. Zhang, N. Noor, S. Alay-e-Abbas, A. Shaukat and R. Khenata, *The half-metallic ferromagnetism character in Be1− xVxY (Y = Se and Te) alloys: An ab-initio study*. J. Magn. Magn. Mater 379 (2015), pp. 63–73.
[45] A. Bourega, B. Doumi, A. Mokaddem, A. Sayede and A. Tadjer, *Electronic structures and magnetic performance related to spintronics of Sr 0.875 Ti 0.125 S*. Opt. Quant. Electron 51 (2019), pp. 385.
[46] K. Yao, G. Gao, Z. Liu and L. Zhu, *Half-metallic ferromagnetism of zinc-blende CrS and CrP: A first-principles pseudopotential study*. Solid State Commun 133 (2005), pp. 301–304.
[47] G. Gao, K. Yao, E. Şaşıoğlu, L. Sandratskii, Z. Liu and J. Jiang, *Half-metallic ferromagnetism in zinc-blende CaC, SrC, and BaC from first principles*. Phys. Rev. B 75 (2007), pp. 174442.
[48] F. Tran and P. Blaha, *Importance of the kinetic energy density for band gap calculations in solids with density functional theory*. J. Phys. Chem. A 121 (2017), pp. 3318–3325.
[49] R. Whited, C.J. Flaten and W. Walker, *Exciton thermoreflectance of MgO and CaO*. Solid. State. Commun 13 (1973), pp. 1903–1905.
[50] B. Doumi, A. Mokaddem, F. Dahmane, A. Sayede and A. Tadjer, *A novel theoretical design of electronic structure and half-metallic ferromagnetism in the 3d (V)-doped rock-salts SrS, SrSe, and SrTe for spintronics*. RSC Adv 5 (2015), pp. 92328–92334.
[51] R. Soulen, J. Byers, M. Osofsky, B. Nadgorny, T. Ambrose, S. Cheng, P.R. Broussard, C. Tanaka, J. Nowak and J. Moodera, *Measuring the spin polarization of a metal with a superconducting point contact*. Science 282 (1998), pp. 85–88.
[52] K. Sato, P. Dederichs, K. Araki, and H. Katayama-Yoshida, *Ab initio materials design and Curie temperature of GaN-based ferromagnetic semiconductors*. Phys. Status Solidi C (2003), pp. 2855–2859.
[53] K. Sato, H. Katayama-Yoshida and P. Dederichs, *Curie temperatures of III–V diluted magnetic semiconductors calculated from first-principles in mean field approximation*. J. Supercond 16 (2003), pp. 31–35.
[54] H. Akai, *Ferromagnetism and its stability in the diluted magnetic semiconductor (In, Mn) As*. Phys. Rev. Lett 81 (1998), pp. 3002.
[55] S. Sanvito, P. Ordejón and N.A. Hill, *First-principles study of the origin and nature of ferromagnetism in Ga 1− x Mn x As*. Phys. Rev. B 63 (2001), pp. 165206.
[56] H. Raebiger, A. Ayuela and R. Nieminen, *Intrinsic hole localization mechanism in magnetic semiconductors*. J. Phys-Condens. Mat 16 (2004), pp. L457.

[57] V.L. Moruzzi, J.F. Janak, and A.R. Williams, *Calculated Electronic Properties of Metals*, Springer Science & Business Media, Pergamon, 1978.

[58] U. Verma, S. Sharma, N. Devi, P. Bisht and P. Rajaram, *Spin-polarized structural, electronic and magnetic properties of diluted magnetic semiconductors Cd1−xMnxTe in zinc blende phase*. J. Magn. Magn. Mater 323 (2011), pp. 394–399.

[59] H. Lakhdari, B. Doumi, A. Mokaddem, A. Sayede, J.P. Araújo, A. Tadjer and M. Elkeurti, *Investigation of the substituting effect of chromium on the electronic structures and the half-metallic ferromagnetic properties of BaO*. J. Supercond. Nov. Magn 32 (2019), pp. 1781–1790.